AIP | Journal of Applied Physics

Narrow band photocurrent response from partially phase separated a-SiN x :H thin films

R. K. Bommali, Shahab Ahmad, Nandlal Sharma, P. Srivastava, and G. Vijaya Prakash

Citation: Journal of Applied Physics **116**, 113501 (2014); doi: 10.1063/1.4895600
View online: http://dx.doi.org/10.1063/1.4895600
View Table of Contents: http://scitation.aip.org/content/aip/journal/jap/116/11?ver=pdfcov
Published by the AIP Publishing

Narrow band photocurrent response from partially phase separated *a*-SiN$_x$:H thin films

R. K. Bommali, Shahab Ahmad, Nandlal Sharma, P. Srivastava,[a] and G. Vijaya Prakash
Nanostech and Nanophotonics Laboratory, Department of Physics, Indian Institute of Technology Delhi, Hauz Khas, New Delhi 110 016, India

(Received 7 July 2014; accepted 2 September 2014; published online 15 September 2014)

We report static and dynamic photocurrent response from sub-stoichiometric *a*-SiN$_x$:H thin films. The photocurrent spectral (PCS) response is peaked in the technologically important optical energy range of 2.2 to 4.5 eV. The transient photocurrent response with prolonged exposure is attributed to reduction in number of charge carriers due to trapping of photo-generated carriers at defect sites. The narrow PCS response is attributed to dominant photo-generation of carriers in the bandtails of stoichiometric Si_3N_4 phase and subsequent transport through the excess Si network.
 [http://dx.doi.org/10.1063/1.4895600]

I. INTRODUCTION

Silicon quantum dots (Si QDs) embedded in a dielectric matrix is an attractive system to leverage useful physical properties arising out of the quantum confinement effect (QCE).[1] Predominantly two materials viz. SiO_2 and recently Si_3N_4 are being considered for the choice of a dielectric matrix. Features like, lower barrier to charge carrier injection into QDs, photoluminescence (PL) over the entire visible range and possibility of obtaining in-situ growth of Si-nanostructures without the requirement of post-treatments make silicon nitride an attractive matrix. Si QDs embedded in Si_3N_4 system is being studied for applications like light emitting devices,[2,3] non-volatile memories[4] and for third generation photovoltaic devices like tandem solar cells[5] and spectral converters.[6] In general, low temperature deposited silicon nitride is a partially phase separated[7] composite of amorphous Si (hereafter *a*-Si:H) inclusions in amorphous hydrogenated silicon nitride (hereafter *a*-SiN$_x$:H). Processing the as-deposited material with suitable post deposition treatments like furnace annealing,[8] swift heavy ion irradiation[9] and rapid thermal annealing[3,8,10] leads to the precipitation of Si QDs in silicon nitride matrix. Though, so far, the stress has been on achieving phase separated Si QDs in Si_3N_4 matrix; recent theoretical[11] and experimental reports[12–14] suggest that isolated QDs may not be very attractive for applications where charge transport is desired. It is also mentioned that conduction may be possible only if the QDs are closely spaced (via tunnelling), or, as we will discuss in the present report, if the matrix is partially phase separated[7] wherein, the excess Si provides the necessary conduction pathways. The partially phase separated *a*-SiN$_x$:H shows interesting properties like excitation energy dependent PL[7,15] and a preferential enhancement in PL upon exposure to hydrogen plasma.[16] Further, results presented here become important considering the recent report by *Kiriluk* et al.,[17] which demonstrates the strong absorptive nature and efficient carrier transport in nanocrystalline *a*-Si:H embedded in amorphous matrices, suggesting the advantage of such materials towards improving solar cell efficiencies.

Interest in Si nanostructures embedded in dielectrics is twofold, studying QCE related luminescence and their passive applications such as photovoltaics.[12,18–24] Majority of the existing reports on the photocurrent properties of these materials are related to SiO_2 host matrix, with very few reports related to Si_3N_4. For example, spin dependent charge transport has been reported for *a*-SiN$_x$:H using photoconductivity measurements[25] and others reporting a blue green sensitivity with Si nanostructures embedded in Si_3N_4.[18,24] It must be noted that the above cited articles reporting photoconductivity measurements were carried out using different electrode materials and measurement geometries, wherein the nature of photocurrent spectral response reported is broadband, ranging from the blue to red part of the visible spectrum.

In the present work, we report the observation of photocurrent spectral response in *a*-SiN$_x$:H thin films of different compositions. The compositional variation of films is expected to bring a variation in the average size of the nanoscale Si inclusions. The photocurrent spectra have interesting features like a predominant UV sensitivity and double peak feature, with negligible response in the red-end spectral region. Here, we attempt to explain the physical origins of these observations, supported from other optical and electrical measurements. In interpreting the results, we continue with the view of Si rich *a*-SiN$_x$:H, as a composite material as presented in our previous publications.[15,16]

II. EXPERIMENTAL DETAILS

Here, we report the static and dynamic photo current response measurements on *a*-SiN$_x$:H thin films, with varying excess Si content, deposited on ITO glass (ITO/g) substrates and on a p-type Si (100) substrate for a selected case. The films were prepared using SiH_4 (4% in Ar) and NH_3 precursor gases by means of plasma enhanced chemical vapour deposition (PECVD). Other deposition parameters: substrate temperature, chamber pressure, and plasma power were 200 °C, 1 mbar, and 25 W, respectively. The photocurrent measurements

[a]Author to whom correspondence should be addressed. Electronic mail: pankajs@physics.iitd.ac.in

were carried out in vertical and lateral geometries. For vertical geometry of photo-electrical measurements, Al coated on top of the film and the ITO/g substrate act as electrodes, whereas for lateral geometry two Al contacts, separated by ~900 μm, were made on top of the films deposited on Si substrates. The investigated films have a thickness of ~100 nm and size of the photoconductive device/cell in the vertical geometry is 2 × 2 mm^2. During photocurrent measurements, Xenon lamp was used as a light source coupled with a Bentham monochromator to facilitate wavelength selection, with a spectral resolution of 0.1 nm. All the electrical characteristics were measured with a μAutolab (type III) galvanostat/potentiostat,which is equipped with a pico-ammeter and a d.c.voltage source (−5 V to +5 V) has been used as potentiostat. The counter electrode and working electrode (joined with reference electrode) from potentiostat have been connected to the film via ITO and Al metal contacts. The partial phase separation and the presence of *a*-Si:H inclusions in the films have been confirmed from XPS and HRTEM respectively, the experimental details of which are discussed elsewhere.[22] The composition of the films was obtained from RBS experiments, carried out using 1.7 MeV He^{2+} ions at a backscattering angle of 170°, with a detector solid angle of 3.052 milli-steradians and a resolution of 17 keV. The optical absorption spectra and the bandgap (E_g) values are obtained from the spectral information obtained from Shimazdu UV3600 spectrophotometer. The thicknesses of the films have been determined using X-ray reflectivity (XRR) measurements with Bruker D8. The analysis of RBS data indicates that the ratio between nitrogen and Si (N/Si ratio) for the films ranges from 0.3 to 1.3 (see Table I). Correspondingly the optical bandgaps (E_g) estimated from absorption spectra vary from 2 eV (approaching a-Si) to 4.5 eV (close to stoichiometric *a*-Si_3N_4).

III. RESULTS AND DISCUSSION

The details of all the films considered in the present work are enlisted in Table I. First, we present the transient photocurrent response of *a*-SiN_x:H film to illumination, by measuring the current across the electrodes at various bias conditions (Figure 1). The results are presented for film S4, other films also exhibit a similar behaviour. Two cases are presented, the blue curve represents the current generated at a bias voltage of near 0 V, the red curve on the other hand is the current generated under a bias of 5 V. Both the curves show an abrupt increase in the current under illumination and a typical ON-OFF mechanism with a clear evidence that the *a*-SiN_x:H films show strong photo carrier generation. In order to understand the measurement process clearly, let us look at

TABLE I. The N/Si ratio and the estimated optical gap values and the thicknesses of *a*-SiN_x:H thin films.

Film	N/Si (x)	Optical gap Eg (eV)	Thickness (nm)
S1	0.3	2	110
S2	0.4	2.1	46
S3	0.5	2.2	118
S4	1.1	3.8	57
S5	1.3	4.5	127

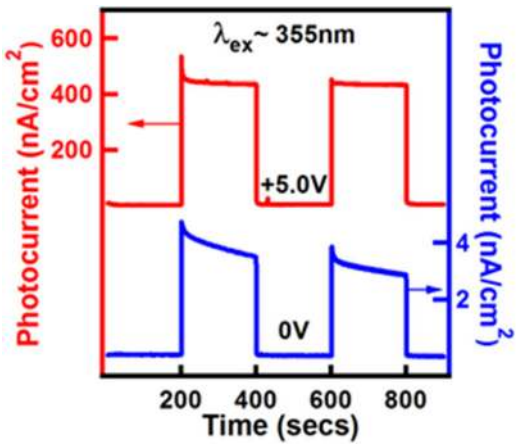

FIG. 1. A typical transient photocurrent response under excitation with 355 nm wavelength for bias voltages 0 V (blue) and 5 V (red). The photocurrent generated for each curve is marked on the Y-axis.

the device geometries used and the corresponding energy band diagrams. The vertical geometry adopted is depicted in Figure 1(a), whose details are provided in the experimental section. Figure 2(b) shows corresponding electronic energy band diagrams, before and after electrical contact. The work function of the electrodes used viz. Al (ϕ_{Al}), ITO (ϕ_{ITO}), and the *a*-SiN_x:H electron affinity ($\chi_{a\text{-}SiNx:H}$) are depicted in these schematics to visualise the modification of the band edges when these layers are brought into electrical contact. As is evident from the Figure 2(b), due to a difference in work functions of ITO and Al, the *a*-SiN_x:H conduction band slopes towards Al after the Fermi levels of Al and ITO align subsequent to an electrical contact between the layers.

The photocurrent spectral (PCS) responses for *a*-SiN_x:H are depicted in Figure 3 for films (S1 to S5) of different compositions. Details of these films are provided in Table I. There are several notable features in these data, which make

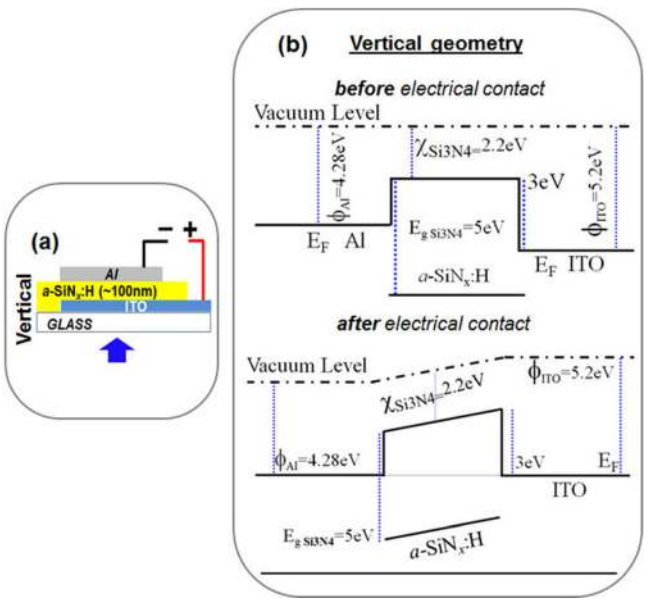

FIG. 2. (a) The vertical geometry adopted for photocurrent measurements. (b) Schematic energy band diagram for vertical geometry before (top) and after (below) electrical contact between the layers.

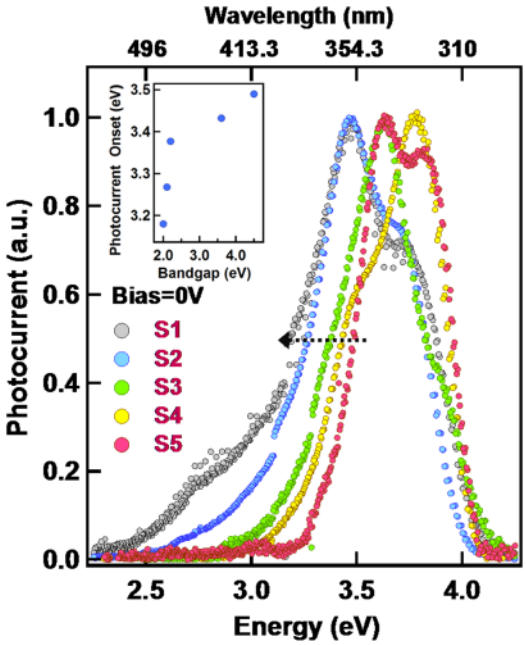

FIG. 3. The normalized photocurrent spectral response for a-SiN_x:H thin films collected under zero bias voltage. Inset shows the plot of blue-shift in photocurrent on-set against the optical bandgap (Eg). The onsets have been taken to be the value of optical energy at mid intensity values (indicated by dotted arrow) of photocurrent.

it interesting and distinct from the spectral response data reported in literature for similar materials. First, it may be noted that PCS response for the films extends from the UV to green region of the visible spectrum. In particular, the PCS is double peaked in the UV-blue region. Second, the response below 2.5 eV is negligible. These features are quite distinct from other competing Si based composites such as Si–nanocrystals embedded in a-Si:H, SiO_2 and Si_3N_4 systems and silicon carbon nitride thin films.[18–21] For example, differences can also be seen in the report by *Torre* et al.,[24] which discusses the comparison of the spectral response from SiO_2 and Si_3N_4 based nanostructured films, wherein a blue peaked response was observed for both the materials. The response was peaked in the blue region with a tailing behaviour that extended into the red region. The UV to green sensitivity of the a-SiN_x:H films thus demarcate the present results from those reported in literature.

As seen from Figure 3, the PCS responses for all the films are maximum at around 3.3 to 4 eV. This behaviour can be understood by considering the fact that the band gap of stoichiometric silicon nitride[26] ranges between 4.5 to 5 eV (Table I), and therefore it may be inferred that band tail states just below the absorption band edge act as centres for the creation of charge carriers under illumination. Further, the role of Si inclusions in the observed features may be ruled out, as their expected response should come in the red region of the spectrum.[27] To elaborate further, if we consider the band gap of quantum confined Si (from *Park* et al.[28]), a sharp response is expected in the UV-blue region for a-Si inclusions having narrow size distribution of ~1.5 nm. However, the films in the present case are partially phase separated with large variation of the sizes (2 to 10 nm) of the a-Si inclusions.[15] Also, the marginal spectral shift in the PCS, despite major compositional variation in the films clearly indicates that the silicon nitride phase in the composite matrix is the major contributor to the observed PCS response. Next, we consider the tailing effect towards the lower energies. The inset in Figure 3 shows the variation of the photocurrent onset with the E_g, wherein we consider the photon energy at which the PCS intensity is half to be representing the onset. This tailing of the PCS can be attributed to the modification of the bandtail states with increasing Si content[26] in random bonded Si rich a-SiN_x:H. It is a reasonable assignment, as the films under consideration are partially phase separated, whereby both random mixed[29] as well as random bonded[30] regions may be expected to be present within the films.[31] Also, the dissipation of the photo-generated carriers into the midgap radiative and non-radiative defects[15] of the silicon nitride matrix cannot be ruled out. Therefore, the low PCS response in the spectral region below 2.5 eV could be an indication of possible dissipation of energy via radiative recombination of charged carriers. While the charge separation in Si QDs may be difficult due to their higher binding energies,[32] excess of silicon content contributes to the photocurrent by providing conduction channels necessary for the transport of carriers photo-generated in Si_3N_4 bandtails. This view is in agreement with our observation that,

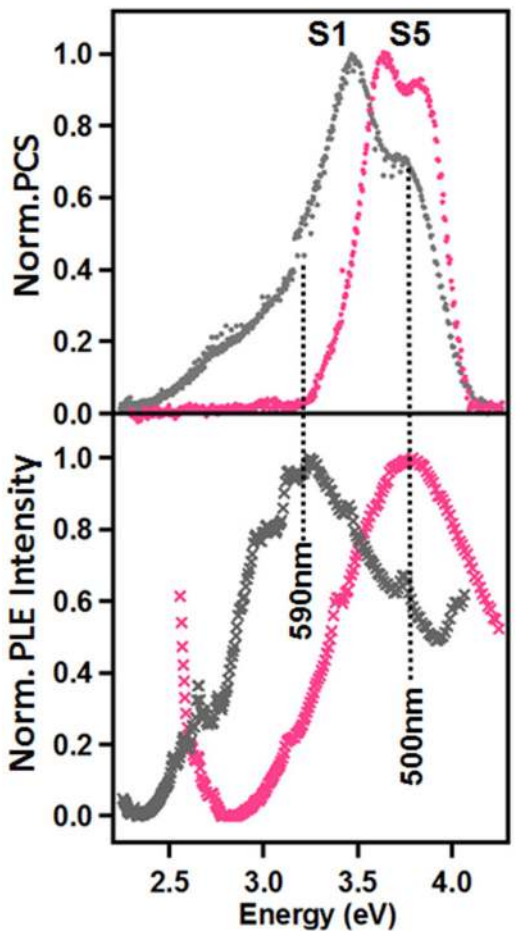

FIG. 4. Comparison of the photocurrent spectral response (top) of films S1 and S5, with the photoluminescence excitation for films similar to S1 and S5 represented by corresponding colours. The PLE monitoring wavelengths were 590 nm and 500 nm as marked against the corresponding curves.

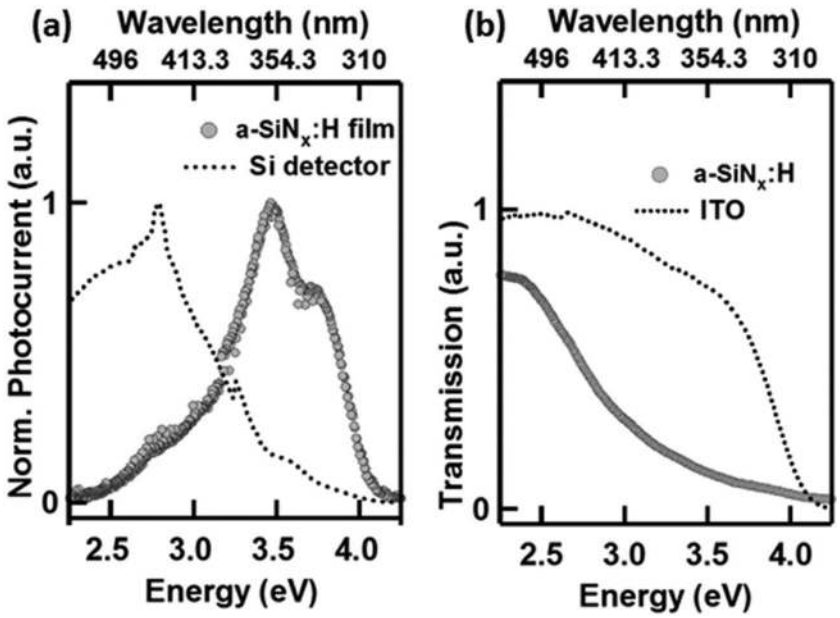

FIG. 5. (a) Comparison of the PCS response of a commercial Si detector (dots) with that of a-SiN_x:H film (circles) using the same experimental set-up. (b) The transmission spectra of a bare ITO coated glass substrate (dots) and the a-SiN_x:H film (circles).

both PL spectra[16] and the photocurrent spectral response are excited in mutually exclusive spectral regions.

The PL from the above mentioned a-SiN_x:H thin films has a broad band nature ranging between 3.2 and 1.5 eV. The broad band response was attributed to the presence of multiple radiative centers like nitrogen dangling bonds, Si dangling bonds, and a-Si inclusions in these films.[15] Further clarity on the photogeneration mechanism is provided by comparison of photoluminescence excitation (PLE) and the PCS data as shown in Figure 4, wherein we compare the extreme films S1 and S5. From the (PLE) measurements (Figure 4), the optimum excitation energies are found to be 3.1 eV and 3.7 eV, respectively, for Si rich (S1) and near stoichiometric (S5) films, which are indeed well within the region of photocarrier generation (3.0 eV to 4.1 eV,) (see Figure 3). Therefore, it can be inferred that radiative recombination (PL) takes place only after photo-generated carriers thermalize down to lowest bandtail states, which in agreement with the present understanding of radiative recombination in amorphous materials.[33]

Now we address the sharp edge in the PCS spectra, above 4 eV. Figure 5(a) shows a comparison of the normalised PCS response of one of the a-SiN_x:H films S1 with the response of a commercial Si detector measured under similar conditions. Here, it should be mentioned that all the films show a similar edge, therefore the following discussion applies to all films. Further, Figure 5(b) also shows the transmission spectra of a typical a-SiN_x:H film and corresponding ITO/g substrate. From Figures 5(a) and 5(b), it is clear that the higher energy edge (~4 eV) of the PCS response could be a manifestation of the ITO/g absorption edge. In order to investigate the role of device geometry and contact related effects, the photocurrent spectra have also been recorded in lateral geometry for an a-SiN_x:H film deposited simultaneously on both ITO/g and Si substrates as shown schematically in Figure 6(a). The PC spectra also show a comparison obtained in both lateral and vertical geometries for one of the films. Along with PC spectra, Figure 6(b) also shows the band diagram corresponding to the lateral device before and after electrical contact. The energy band structure does not change after electrical contact because of the Al on the either sides of a-SiN_x:H; as the Fermi levels are already aligned. It can be noticed from Figure 6(c) that the PC spectra recorded in different geometries are comprised of two peak structure with different relative amplitudes. Thus confirming that the observed spectral response is an intrinsic nature of a-SiN_x:H thin films and is independent of device geometry. It may also be noticed that the photocurrent amplitudes measured in the lateral geometry are relatively smaller compared to that in the vertical geometry, which could be due to differences between the overall charge carrier transport lengths before collection at the electrodes.

We now describe the results that throw light on the double peak feature noticed in the PCS data. Figure 7(a) shows the PCS measurements at different bias voltages. It may be

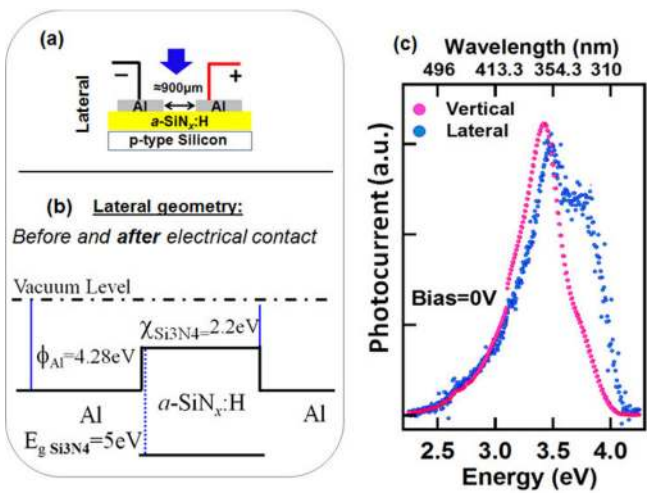

FIG. 6. (a) The schematic of the Lateral geometry adopted for film deposited on Si substrate and (b) schematic energy band diagram. (c) The normalised PCS response of a-SiN_x:H film for lateral (blue dots) and vertical (pink dots) geometries, respectively.

observed that the photocurrents are increasing with the increasing of bias voltage. This result can be attributed to the enhancement in the population of energy levels with photo-generated carriers. Evidence of which is also observed in the transient photocurrent data presented in Figure 1. This is elaborated as follows: according to the typical photocurrent transient response characteristic shown in Figure 1, the photocurrent response gradually decreases with increasing duration of the light exposure. Having used very low light powers, such behaviour can be expected when there are traps/defects that lead to a decrease in the number of photo-generated carriers. These defects can be present at the *a*-Si:H/*a*-SiN_x:H interfaces. Specifically, the fall in photocurrent in the ON state can be attributed to charging of defects, as observed by Koyanagi *et al.*[12] in photo-capacitance measurement, wherein the transient behaviour has been associated with the presence of *a*-Si phase within SiO_x thin films.

In the present experiment, the photocurrent decay under illumination is however found to diminish when an external bias is applied (see Figure 1). This is attributed to the additional photogenerated carriers generated in the presence of an external bias as it aids charge separation. The normalised PC spectral data (Figure 7(b)) show a clear change in spectral shape going from the bias voltages of 0 V to 1 V. It must be noted that the zero bias condition corresponds to small

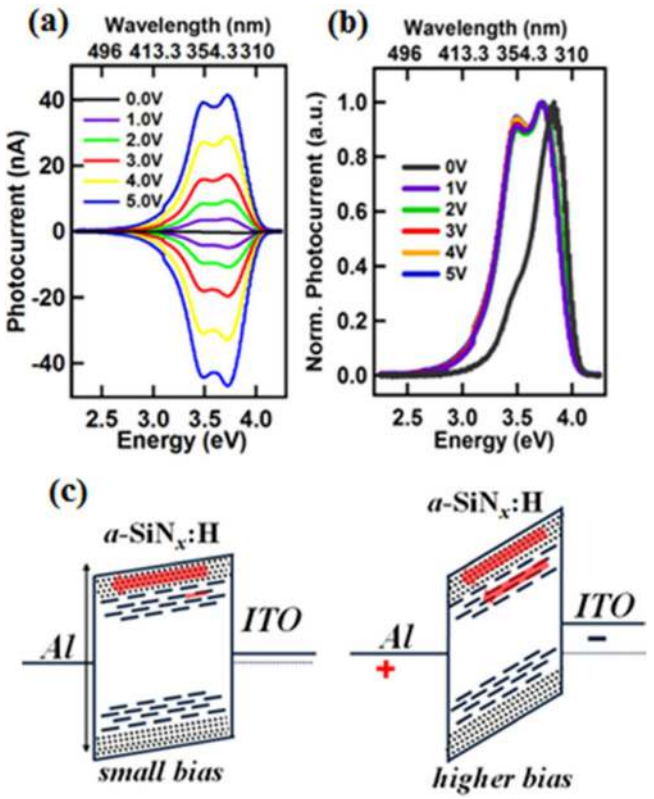

FIG. 7. (a) The evolution of photocurrent spectra for film S4 with applied bias voltage from 0 (~1 mV) to 5 V. (b) shows the corresponding normalised spectra. Upon application of a bias, the contribution of lower energy states to the photo carriers increases. (c) Schematic showing the photo-generated carrier transport through two sets of band tail states under a small bias (~1 mV) (left) and a higher bias (right). The states closer to the conduction band have lower localisation (dotted), whereas deeper states have higher localisation (dashed).

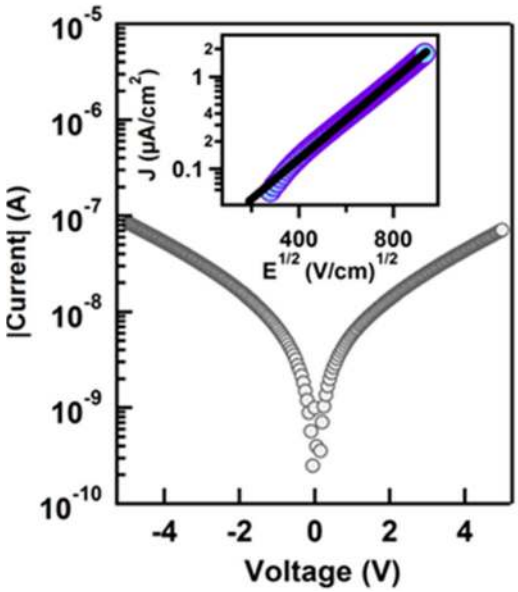

FIG. 8. The typical Current-Voltage (IV) graph under illumination with 355 nm. Inset shows a linear fit to the plot of current density versus the square root of electric field, there by indicating that the Poole-Frenkel mechanism is responsible for photo-conduction.

but finite voltage of less than 1 mV. This change in spectral shape is understood in the following manner; under a low bias voltage condition, the photo-carrier generation takes place (or preferred) in the band tails states close to the band edges, however the increase of bias voltage tends to increase the participation of states further below the band edge. The increase in photo-carrier generation in energetically low-lying band tail states can be understood from the schematic band diagram shown in Figure 7(c) for a vertical geometry photocurrent device. It is well known that the degree of localisation of bandtail states increases as one moves deeper into the gap,[34] and with this understanding it may be appreciated that the transport across states with high localisation would be relatively difficult compared to states with low localisation in space. In the present case, therefore, the application of an external bias facilitates the transport and subsequent collection of photo-generated carriers across deeper bandtails (see Figure 7(c)).

Further, information on the carrier transport mechanism is revealed by the current-voltage (I-V) measurements. Figure 8 shows the typical I-V characteristics for one of the of *a*-SiN_x:H thin film (S5) under illumination with 355 nm wavelength from the Xe light source, wherein the current response exhibits an exponential rise with increase in voltage. Further insight into the conduction mechanism is provided by the inset graph showing a plot of current density (J) versus the square root of applied electric field ($E^{1/2}$). The convincing linear fit of experimental data corroborates that the photo-transport occurs via the Poole-Frenkel conduction mechanism, characteristic of amorphous materials.[35]

IV. CONCLUSIONS

In conclusion, the UV-visible spectral photo-sensitivity is observed in *a*-SiN_x:H thin film devices, in which the of

a-SiN_x:H is partially phase separated composite of a-Si:H and a-SiN_x:H. This UV sensitivity results from the generation of carriers in the band tails of the Si_3N_4 phase as evident from the PL and PLE data. The Si rich regions present in the films are believed to promote the transport of these carriers to the collecting electrodes before they recombine. On the other hand, the carriers photo-generated in the Si rich regions of the matrix are found to recombine via radiative recombination, thereby leading to the absence of the PCS amplitudes in the red region of the spectrum. The transient photocurrent experiments show the trapping of charge carriers by defects. However, trapping of carriers by defects can be overcome by increasing the bias, which enhances the carrier transport from the low lying bandtails below the conduction band edge. The prominent double peak feature in all the photocurrent spectral data is attributed to contribution from the photocurrent from sub-bands in the bandtail states of a-SiN_x:H having different degrees of localization. However, a complete understanding of these sub-bands would require detailed investigations.

ACKNOWLEDGMENTS

One of the authors R.K.B. is thankful to the Council of Scientific and Industrial Research CSIR), New Delhi for providing financial support. This work was supported by High-Impact Research Scheme of IIT Delhi, UKIERI, and Nanoscale Research Facility of IIT Delhi. The XRD Central facility of IIT Delhi is acknowledged for the XRR measurements.

[1]L. T. Canham, Appl. Phys. Lett. **57**, 1046 (1990).
[2]Z. H. Cen, T. P. Chen, Z. Liu, Y. Liu, L. Ding, M. Yang, J. I. Wong, S. F. Yu, and W. P. Goh, Opt. Express **18**, 20439 (2010).
[3]J. Warga, R. Li, S. N. Basu, and L. D. Negro, Appl. Phys. Lett. **93**, 151116 (2008).
[4]E. Kim, T. Yim, S. An, W. J. Cho, and K. Park, Appl. Phys. Lett. **97**, 222107 (2010).
[5]P. D. Nguyen, D. M. Kepaptsoglou, Q. M. Ramasse, and A. Olsen, Phys. Rev. B **85**, 085315 (2012).
[6]X. Huang, S. Han, W. Huang, and X. Liu, Chem. Soc. Rev. **42**, 173 (2013).
[7]L. V. Mercaldo, E. M. Esposito, P. D. Veneri, B. Rezgui, A. Sibai, and G. Bremond, J. Appl. Phys. **109**, 093512 (2011).
[8]B. S. Sahu, F. Delachat, A. Slaoui, M. Carrada, G. Ferblantier, and D. Muller, Nanoscale Res. Lett. **6**, 178 (2011).
[9]S. P. Singh, S. Ghosh, G. VijayaPrakash, S. A. Khan, D. Kanjilal, A. K. Srivastava, H. Srivastava, and P. Srivastava, Nucl. Instrum. Methods B **276**, 51 (2012).
[10]L. V. Mercaldo, E. M. Esposito, P. D. Veneri, G. Fameli, S. Mirabella, and G. Nicotra, Appl. Phys. Lett. **97**, 153112 (2010).
[11]J. W. Luo, P. Stradins, and A. Zunger, Energy Environ. Sci. **4**, 2546 (2011).
[12]E. Koyanagi and T. Uchino, Appl. Phys. Lett. **91**, 041910 (2007).
[13]I. Balberg, J. Appl. Phys. **110**, 061301 (2011).
[14]P. Manousiadis, S. Gardelis, and A. G. Nassiopoulou, J. Appl. Phys. **111**, 083536 (2012).
[15]R. K. Bommali, S. P. Singh, S. Rai, P. Mishra, B. R. Sekhar, G. Vijaya Prakash, and P. Srivastava, J. Appl. Phys. **112**, 123518 (2012).
[16]R. K. Bommali, S. Ghosh, G. Vijaya Prakash, K. Gao, S. Zhou, S. A. Khan, and P. Srivastava, J. Appl. Phys. **115**, 053525 (2014).
[17]K. G. Kiriluk, J. D. Fields, B. J. Simonds, Y. P. Pai, P. L. Miller, T. Su, B. Yan, J. Yang, S. Guha, A. Madan, S. E. Shaheen, P. C. Taylor, and R. T. Collins, Appl. Phys. Lett. **102**, 133101 (2013).
[18]S. K. Kim, C. H. Cho, B. H. Kim, S. J. Park, and J. W. Lee, Appl. Phys. Lett. **95**, 143120 (2009).
[19]C. W. Chen, C. C. Huang, Y. Y. Lin, W. F. Su, L. C. Chen, and K. H. Chen, Appl. Phys. Lett. **88**, 073515 (2006).
[20]O. A. Golikova and M. M. Kazanin, Semiconductors **34**, 737 (2000).
[21]O. Wolf, O. Millo, and I. Balberg, J. Appl. Phys. **113**, 144314 (2013).
[22]R. R. Koropecki, J. A. Schmidt, and R. Arce, J. Appl. Phys. **91**, 8965 (2002).
[23]J. Torre, A. Souifi, A. Poncet, G. Bremond, G. Guillot, B. Garrido, and J. Morante, Solid-State Electron. **49**, 1112 (2005).
[24]J. Torre, G. Bremond, M. Lemiti, G. Guillot, P. Mur, and N. Buffet, Thin Solid Films **511–512**, 163 (2006).
[25]S. Y. Lee, S. Y. Paik, D. R. McCamey, J. Hu, F. Zhu, A. Madan, and C. Boehme, Appl. Phys. Lett. **97**, 192104 (2010).
[26]J. Robertson, Philos. Mag. **63**, 47 (1991).
[27]B. Rezgui, F. Gourbilleau, D. Maestre, O. Palais, A. Sibai, M. Lemiti, and G. Bremond, J. Appl. Phys. **112**, 024324 (2012).
[28]N. M. Park, T. S. Kim, and S. J. Park, Appl. Phys. Lett. **78**, 2575 (2001).
[29]H. R. Philipp, J. Non-Cryst. Solids **8–10**, 627 (1972).
[30]R. Kärcher, L. Ley, and R. L. Johnson, Phys. Rev. B **30**, 1896 (1984).
[31]V. A. Gritsenko, Phys. Usp. **51**, 699 (2008).
[32]K. Y. Kuo, P. R. Huang, and P. T. Lee, Nanotechnology **24**, 195701 (2013).
[33]F. Giorgis, C. Vinegoni, and L. Pavesi, Phys. Rev. B **61**, 4693 (2000).
[34]H. Kato, N. Kashio, Y. Okhi, K. S. Seol, and T. Noma, J. Appl. Phys. **93**, 239 (2003).
[35]R. M. Hill, Philos. Mag. **23**, 59 (1971).